DISSOLUTION OF WASTE GLASSES IN HIGH ALKALINE SOLUTIONS

SEKA SIMPLICE KOUASSI, JONAS ANDJI*, JEAN-PIERRE BONNET, SYLVIE ROSSIGNOL

Groupe d'Etude des Matériaux Hétérogènes (GEMH-ENSCI)
Ecole Nationale Supérieure de Céramique Industrielle, 47-73 Avenue Albert Thomas, 87065 Limoges, France
**Laboratoire de Chimie des Matériaux Inorganiques (Université de Cocody-Abidjan),*
22 BP 582 Abidjan 22, Ivory Coast

E-mail: sylvie.rossignol@unilim.fr

Submitted December 8, 2009; accepted April 27, 2010

Keywords: Glass, Corrosion, Silicate, Water glass, Mineral binder

The aim of this work was to contribute to the dissolution behavior by dissolving waste glass in high alkaline solution. To understand the dissolution behavior, the effect of temperature, particle size distribution, stirring and the nature of the alkaline solution were performed as a function of time. The experiments based on gravimetric, elementary and differential thermal analysis, and SEM measurements showed that all considered parameters displayed the same feature and could be due to a fast ion exchange and a diffusion mechanism associated with the back precipitation of silica species. The alkali cation size played also a role on the dissolution mechanism.

INTRODUCTION

Globally, cement production contributes up to 5 % of CO_2 emissions and uses 1.6 % of electricity consumption. This environmental impact has encouraged research into new low-cost mineral binders to limit CO_2 production and decrease energy consumption. The new alternatives include geopolymers [1] and sodium silicate solution, which are useful in bonding and coating applications.

Glass recycling in housing construction is an innovative approach, and its broad possibilities include the re-use of waste glass as cullet in glass production, as raw material for the production of abrasives as in sand-blasting, and as an aggregate substitute in concrete [2,3]. Glass powders can be used as lubricants, core additives and fluxes in metal foundry work fabrication, and as flux/finders in the ceramics industry. Due to the limited number of industries in Abidjan, all these beneficial usages of waste glass seem very difficult to implement. Indeed, in Abidjan (Côte d'Ivoire), almost 5 000 tonnes of waste glass from commercial sources are generated annually, without including the significant quantity of domestic waste glass. All of this glass is treated as garbage, and none is recycled.

One innovative idea for recycling the waste glass is to use it to synthesize a new mineral binder for particular applications by dissolving it in an alkaline solution.

The chemical reactions involved in glass corrosion have been known for a long time. They include two general concepts. The first is an ion exchange process or the removal of soluble glass constituents (leaching). This reaction takes place in an acid and neutral solutions between the protons of the solution and the alkalis of the glass, leaving the silica structure more or less intact [4] [5]. In an acid solution, the attack rate of the glass is less influenced by the pH of the solution. The glass solubility is constant when the pH value ranges from 2 to 8 [6]. The rate of attack is proportional to the square root of time [4] [7]. The second concept is the glass network dissolution in alkaline solution (etching). All the glass components are released in solution when there is no build-up of insoluble reaction products on the surface. This reaction is controlled by a linear time dependence [7]. The relative importance of that reaction depends on both the glass composition and the corrosion condition. The addition of CaO to binary alkali silicate glass is known to increase its durability [8,9], when the alkaline content enhances the glass dissolution. According to Helebrant [10], the precipitation of species on glass surface could be divided into two parts: the back precipitation of species originally contained in glass and the precipitation of solution species. The first case occurs during the corrosion of glasses containing alkaline earth in distilled water. Layers rich on Mg, Ca and Si were found on glass

surfaces. There are two possible mechanisms of creation of this layer. First mechanism considers that due to the glass dissolution and interdiffusion the ion activity products in respect to mentioned silicates exceeded their solubility products. The precipitated layer is then created through the solution. Second possibility assumes direct reaction of Ca and Mg ions in gel layer on glass surface created. Dissolution of glass in alkaline solution until pH value 10 has been sufficiently performed [11,12]. At high pH value (> 13), the law of glass dissolution versus time could be different.

This paper deals with the dissolution of waste glass in high alkaline solution concentration (> 13). In order to understand the role played by the nature of the solution, the temperature, the particle size distribution and stirring), and the filtrate and glass residue obtained were analyzed by ICP, IR, DTA, XRD and SEM measurements.

EXPERIMENTAL

Materials

The waste glass used in this study was provided by two companies in Abidjan (Côte d'Ivoire). Regarding abbreviations used, SB and SM are bottles glasses obtained from SOLIBRA (Rue du canal, Zone 3, 01 BP 1304 abidjan 01 - Côte d'Ivoire) and VC is window glass from SIVIMI (01 BP 1310 abidjan 01). They were typical soda lime glass. All the samples were broken and washed three times with distilled water. The broken glass was dried in the open air. Then, samples were crushed and sieved to sepa-rate the particles into the following size distributions: >800 μm, 250-800 μm, and 100-250 μm.

Protocol of dissolution

The alkaline solutions were prepared by dissolving analytical reagent-grade sodium or potassium hydroxide in distilled water (0.5 to 5 M). A quantity of the crushed glass (2g) was introduced into polyethylene vessels. Then, 30 ml of alkaline solution was added to each vessel with a mass/volume ratio equal to 0.067. The entire vessel was closed and then baked in an oven at different temperatures under static conditions. Each week, one vessel was removed and the mixture was filtered through a membrane filter with a pore size of 40μm, then washed with water, and dried at 50°C for 14 hours.

In order to identify the role of all parameters, the following nomenclature was used to indicate the residue and filtrate at t time ($^{st}_{G}M^{C}_{T}{}_{t}$) where M, st, G, C, T and t designated respectively the sample code, the stirring, the particles size (μm), the alkaline concentration (mol/l), the temperature (°C) and the time (days). For example, this nomenclature: $_{250\text{-}800}SB_1{}^{70}{}_{14}$ means that the glass used was SB with a particle size of 250-800μm, a concentration of 1 mol/l, a reaction temperature of 70°C and a time of 14 days.

After drying the residues, the weight was determined and the weight loss was calculated by the Equation (1):

$$w_{loss} = \frac{m_0 - m_t}{m_0} \quad (1)$$

where m_0 was the initial weight of the crushed glass (~2g) and m_t was the residue weight at t time. The weight loss according to Equation (1) is in fact given by difference between glass dissolution and back precipitation. However, assuming that the amount of precipitate is much smaller compared to the dissolved glass, this can be used as the measure for the glass dissolution process.

Characterization techniques

The elementary analysis of the diluted solution and the glass residue was estimated by ICP measurement. The mineralization of 20 mg of residue was performed in a CEM microwave MARS 5 using a solution containing 3 ml HF 28%, 3 ml HCl 37% and 1 ml of HNO_3). The apparatus used, IRIS reference, was produced by the firm THERMO JARREL (Cheshire, England).

DTA coupled with TGA was carried out using SETARAM instruments of the SETSYS 24 series. The DTA scans were recorded using a heating rate of 5°C/min under air between 30 and 1200°C in a platinum crucible and using the same amount of alumina powder as the reference material.

SEM was carried out with STEREOSCAN 260 apparatus operating between 10 and 30 kV and linked with an EDS detector. Before the SEM investigation, samples were coated with carbon in an evaporator vacuum.

The IR analysis was done in a Fourier transform spectrometer (Nicolet 380). The samples were dried in the oven for 24 hours at 110°C and about 5 mg were mixed with 100 mg of dried KBr. Spectra were recorded from 4000 to 400 cm^{-1} with 32 scans and a resolution of 4 cm^{-1}.

RESULTS AND DISCUSSION

Nature and concentration effects of the alkaline solution

The degradation of $_{250\text{-}800}SB_1{}^{70}$ in the time in function of the nature of the alkaline solution was shown at Figure 1. Whatever the alkaline solution, an increase of weight loss occurs in function of time. However, the weight loss of SB was higher with the NaOH solution than with the KOH solution, showing the role played by the alkaline cation due to this size. The Na^+ diffusion was slowed down by the K^+ ion, inhibiting the glass dissolution.

For a given alkaline solution, the degradation rate of SB increased slightly with the concentration (Figure 2). This behavior has also been reported in other studies.

Effectively, when the concentration of the alkaline solution was multiplied by 2 or by 10, the dissolution rate was multiplied by 1.1 or by 1.5 respectively.

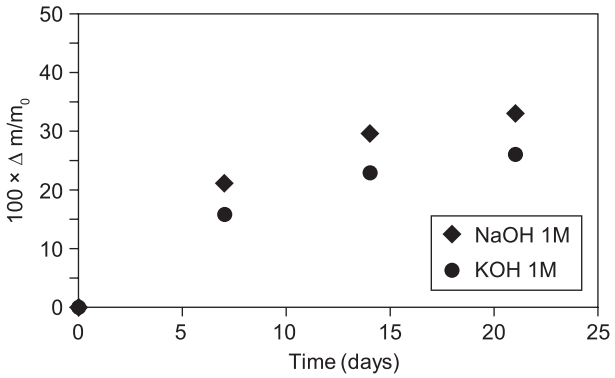

Figure 1. Weight loss of SB versus time in function of the nature of alkaline solution (NaOH and KOH) in for $_{250\text{-}800}SB_1^{70}$ conditions.

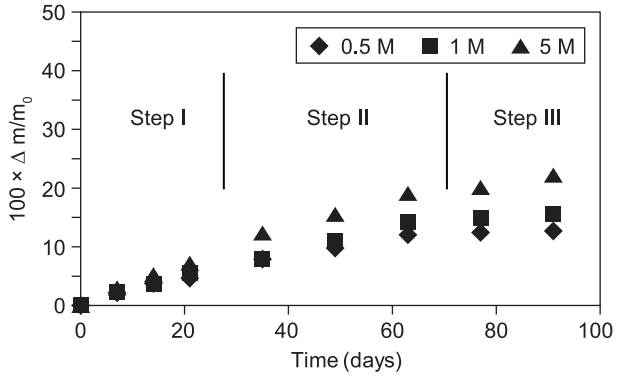

Figure 2. Weight loss of SB versus time in function of the concentration of alkaline solution (NaOH) for $_{250\text{-}800}SB^{70}$ conditions.

The dissolution curves could be divided into three steps (Figure 2). Step I consisting of a linear range in function of time, could be explained by a glass network dissolution which is not influenced by solution saturation or by precipitation of dissolved glass components and/or solution components on the surface. The second step, where the dissolution slow down can be due by both the back precipitation of the silica and the saturation of solution. The last step can be explained by the presence of carbonate species which deposited at the surface inhibiting the dissolution and the ions silicate transport. However, these interpretations would be compared with results obtained from bulk glasses dissolution in a same alkaline solution. Bunker [9] explained that the tetrahedral SiO_4 sites common to all silicates glasses were susceptible to nucleophilic attack primarily by OH^- to form a reactive five-coordinated intermediate which can be decomposed to rupture the Si–O–Si bond (Eq. (2)).

$$\begin{array}{c} \text{OH} \qquad\qquad\quad \text{OH} \\ \text{Si–O–Si–OH} + \text{OH} \longrightarrow \text{Si–O–Si–OH} \longrightarrow \text{Si–O}^- + \text{Si(OH)}_4 \\ \text{OH} \qquad\qquad\quad \text{OH}\ \ \text{OH} \end{array} \qquad (2)$$

Therefore, a significant quantity of OH^- could improve the formation of a five-coordinated intermediate which could lead to a great dissolution of the glass.

Effect of the temperature and particle size distribution

Figure 3 shows the weight loss curves of SB versus time in function of the reaction temperature. An increase of temperature induced an increase of dissolution since a variation of 20°C induced a dissolution rate multiplied by 3. This result was in good agreement with the concept [4], which previewed a factor of 1.5 to 2.0 per 10°C due to the increase of the ion diffusion in relation to the energy of activation. Figure 4 indicates the weight loss curves of SB versus time in function of the particle size distribution. For a given time, the weight loss increased when the particle size distribution decreases; the dissolution rate was multiplied by 3, and by 2.2 when the range changed from > 800 to 250-800 μm and 250-800 to 100-250 μm, respectively. These results are in relation with an increase of surface reactivity linked to specific surface area of glass.

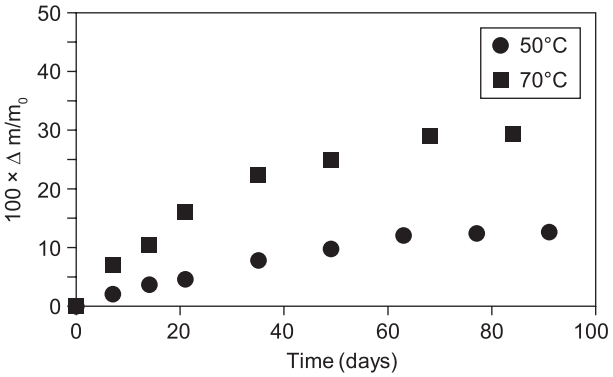

Figure 3. Weight loss of SB versus time in function of the temperature for $_{250\text{-}800}SB_{0.5}^{50}$ and $_{250\text{-}800}SB_{0.5}^{70}$.

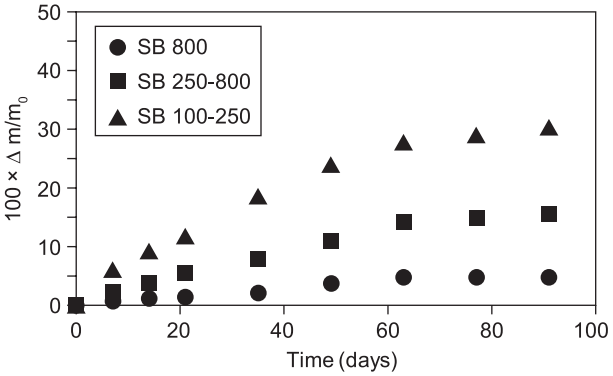

Figure 4. Weight loss of SB versus time in function of the particle size distribution for SB_1^{50}.

In all cases, the dissolution rate decreased with time and tended to become constant for a long time, meaning that total dissolution of the glass was prevented.

Effect of the chemical composition of the glass

The chemical composition of SB, SM and VC determined by ICP measurements expressed in weight percentage of oxide is reported in Table 1. The major elements of the three samples were: SiO_2, Na_2O and CaO, and their compositions were almost the same, except the CaO content, which was lower for VC.

Table 1. Chemical composition of SB, SM and VC (wt.%).

	Al_2O_3	CaO	Fe_2O_3	K_2O	MgO	Na_2O	SiO_2	TiO_2
SB	1.64	9.19	0.23	0.56	0.84	13.89	73.37	0.28
SM	1.13	9.43	0.09	0.27	1.29	14.64	72.98	0.17
VC	1.23	7.20	0.15	0.32	3.93	14.99	71.09	0.11

The evolution of the dissolution rate of SB, VC and SM versus time (Figure 5) shows that the dissolution rate of SB was smaller than those of VC and SM, which were similar. The same reactivity of VC and SM could be explained by a significant quantity of alkaline-earth ions (Table 1) influencing the dissolution of the glass [9].

Effectively, the glass network hydrolysis was more rapid when non-bridging oxygen atoms were present. Site reactivity followed the trend Q1 > Q2 > Q3 > Q4 where Q refers to the number of bridging oxygen atoms [13]. The total number of non-bridging oxygen atoms increased with the modifier content of the glass. According to this effect, the reactivity of the samples where the molar ratios of $(Na_2O+K_2O)/SiO_2$ were 0.21, 0.20 and 0.19 for VC, SM and SB, respectively were in agreement with the results. Moreover, glass samples with high CaO and MgO contents were known to enhance corrosion resistance [8] [9]. The glass alkaline and alkaline earth content created an opposite competition on the glass reactivity.

Filtrate and residue analysis

Figure 6 shows the Si molar fraction dissolved versus time for different filtrates depending on particle size distribution. As the weight loss of SB, the Si fraction dissolved in solution increased versus time and tended to stabilize. The total mole number of Si, Na and Ca was determined before and after glass dissolution in order to determine the ICP measurement error of each element (Table 2). The uncertainty of ICP measurement on silicon was almost 10%. At the end of the experiment, the ratio n_{Si}/n_{Na} was different in the residue and in the filtrate in relation to initial composition, suggesting an incongruent dissolution according to previous works [6].

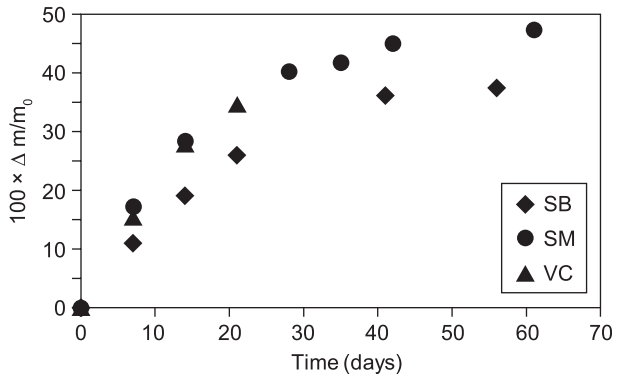

Figure 5. Weight loss versus time of SB, SM and VC (G = 250-800 μm, T = 70°C and [NaOH] = 1M).

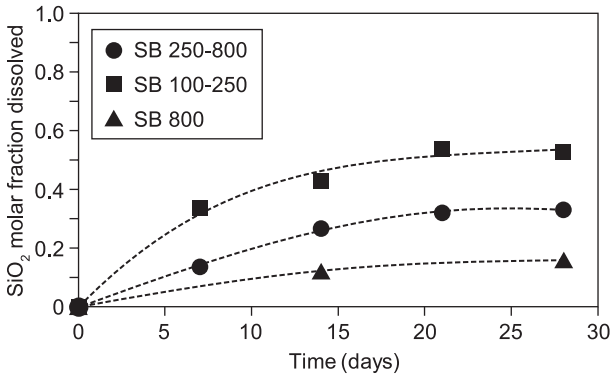

Figure 6. Evolution of SiO_2 in the filtrate SB_1^{70} versus time for various size distributions.

Table 2. Moles number of Si, Na, Ca and Mg in 1 g of SB and 15mL of NaOH solution before and after alkaline attack.

	Initial products			Final products		
$_{250\text{-}800}SB_1^{70}{}_{28}$	SB	NaOH	total	residue	solution	total
n_{Si}/moles	1.24×10^{-2}	0	1.24×10^{-2}	8.25×10^{-3}	5.15×10^{-3}	1.34×10^{-2}
n_{Na}/moles	4.48×10^{-3}	1.5×10^{-2}	1.95×10^{-2}	3.02×10^{-3}	1.62×10^{-2}	1.92×10^{-2}
n_{Ca}/moles	1.64×10^{-3}	0	1.64×10^{-3}	1.74×10^{-3}	2.33×10^{-6}	1.74×10^{-3}
n_{Mg}/moles	2.08×10^{-4}	0	2.08×10^{-4}	1.75×10^{-4}	0	1.8×10^{-4}
n_{Si}/n_{Na}	2.77		0.64	2.73	0.32	

Glass residual characterization

In order to understand the phenomenon attributed to the partial dissolution rate of SB, micro structural studies conducted by SEM of the glass, before alkaline attack and $_{250\text{-}800}SB_1{}^{70}{}_{28}$ were performed (Figure 7) and provided evidence of the formation of some species at the glass surface during the alkaline attack. Those species prevented contact of the alkaline solution and the glass network and were attributed to the precipitation of the alkaline earth silicates [6, 10].

Infrared spectra of fresh glass and residue $_{100\text{-}250}SB_1{}^{70}{}_{28}$ were given in Figure 8. For the fresh glass, the main bands centered at around 3500, 1010 and 770 cm^{-1} could be attributed to SiO-H [14], Si-O-Si asymmetric stretching [15, 16] and Si–O–Si bending vibration [17], respectively. The spectrum of the $_{100\text{-}250}SB_1{}^{70}{}_{28}$ sample displayed additional peaks due to the hydratation mechanism with a peak located at 1634 cm^{-1} assigned to the bending vibration of H_2O [18] and to a carbonated surface with peaks at 1423, 1494 and 684 cm^{-1} assigned to the C–O vibration of the carbonate ion [19].

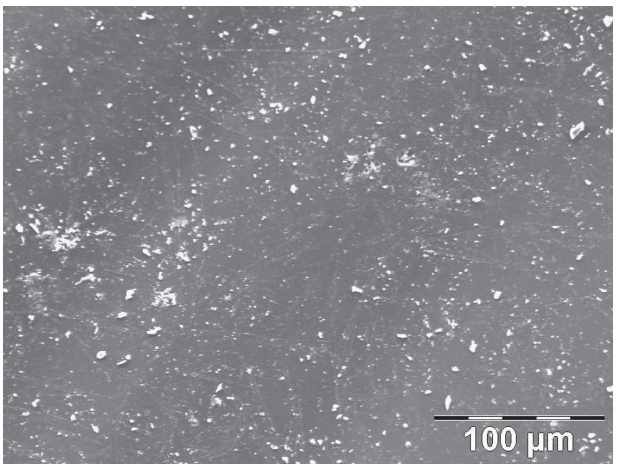

a) fresh SB

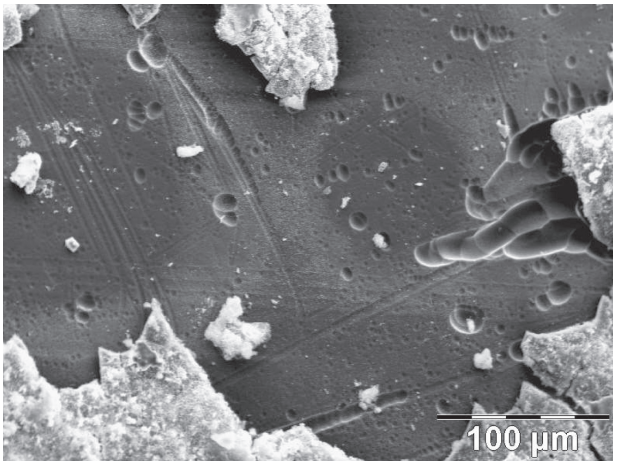

b) $_{250\text{-}800}SB_1{}^{70}{}_{28}$

Figure 7. SEM micrographs of SB.

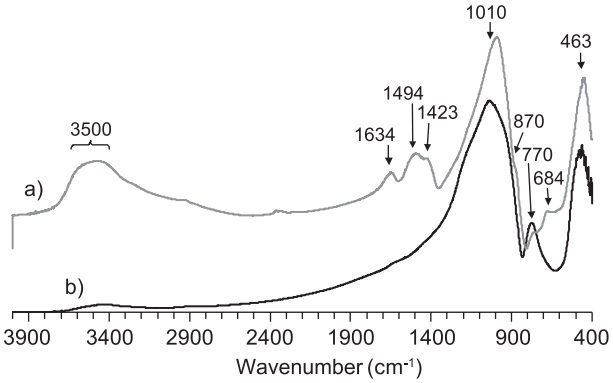

Figure 8. FTIR absorption spectra of: a) fresh SB, b) after alkaline attack $_{100\text{-}250}SB_1{}^{70}{}_{28}$.

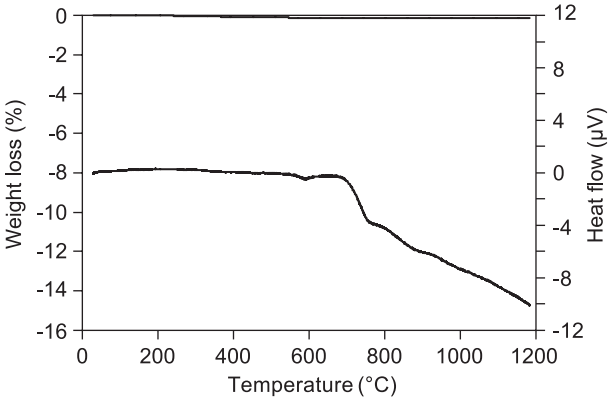

a) fresh SB

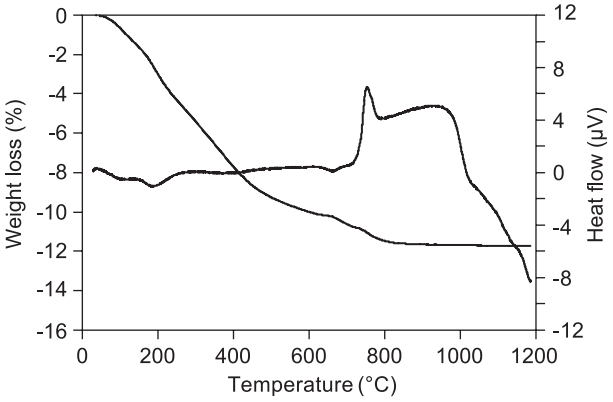

b) $_{250\text{-}800}SB_1{}^{70}{}_{28}$

Figure 9. DTA and TGA curves of SB.

Otherwise, the thermal curves of the fresh glass (Figure 9a) indicated an athermic event at 600°C, characteristic of the glass transition temperature always presented in Figure 9a. However, some endothermic or exothermic peaks linked to weight loss could also be observed after washing with water (Figure 9b). The endothermic peaks below 400°C were due to physical or bulk water [20]. The exothermic peak at 750°C was

assigned to the elimination of some carbonated species on the surface of the glass residue due to the alkaline medium. The exothermic peak at around 970°C may have been due to some crystallization but was not confirmed. All these results were in good agreement with FTIR results.

CONCLUSIONS

The dissolution of three kinds of glass (SB, SM and VC) was studied in alkaline solution at different temperatures and concentrations, and with different particle size distributions. The main results show that although the dissolution rate of the glass was greatly influenced by the temperature of the reaction, the glass composition, and the particle size distribution, it depended fairly by the alkaline solution concentration. The dissolution rate was also influenced by alkaline cation in the etching solution. The decreasing time dependence of dissolution curves can be explained by the formation of precipitated layer on the glass surface. The characterization of filtrate and residue were in agreement with these hypotheses.

References

1. Davidovits J.: *Geopolymer - chemistry and applications*, 2nd ed., p.3-17, Institute of Geopolymer, France 2008.
2. Guohua C., Harry L.: Waste Management *22*, 747 (2002).
3. Yixin S., Thibaut L., Shylesh M., Damian R.: Cement and Concrete Research *30*, 91 (2000).
4. Mc.Lellan G. W.: *Glass Engineering Handbook*, Mc Graw-Hill, New York 1984.
5. Zarzycki J.: *Les verres et l'état vitreux* , édition Masson, p.347-350, Paris 1982.
6. Barton J.: *Le verre, science et technologie*, EDP sciences, p.162-170, France 2005.
7. Hench, L. L: J. Non-Cryst. Solids. *25*, 343 (1977).
8. Paul A.: *Chemistry of glass*, 2nd ed., p.188-202, Chapman and Hall, New York 1990.
9. Bunker B.C., D.R. Tallant, T.J. Headley, G.L. Turner and R.J. Kirkpatrick: Chemistry of glasses. *29*, 106 (1988).
10. Helebrant A.: Ceramics-Silikaty *41*, 147 (1997).
11. Strachan D. M. in: Nuclear Waste Management (Ed.: Wicks G. G., Ross W. A., The Am.Ceram.Soc., Columbus, Ohio 1983.
12. McCoy J. K., Markworth A. J.: J. Non-Cryst. Solids *89*, 47 (1987).
13. Engelhardt G., Zeigan D., Jancke H., Hoebbel D., Wieker W.: Z. Anorg. Allg. Chem. *418*, 17 (1975).
14. Bartholomew R. F., Butler B. L., Hoover H. L., Wu C. K.: J. Am. Ceram. Soc. *63*, 481 (1980).
15. Park E. S., Ro H. W., Nguyen C. V.: Chem. Mater. *20*, 1548 (2008).
16. Brown J. F.: J. Am. Chem. Soc. *87*, 4317 (1965).
17. Petre M., Gligor J., Branko K.: J. Mol. Str. *942*, 413 (2009).
18. Innocenzi P.: J. Non-Cryst. Solids *316*, 309 (2003).
19. Pajares I., Martinez-Ramirez S., Blanco-Varela M. T.: Cement and Concrete Composites *25*, 861 (2003).
20. Mounanga P.: PhD Thesis, Université de Nantes 2003.